

A Mouse Model for the Carney Complex Tumor Syndrome Develops Neoplasia in Cyclic AMP–Responsive Tissues

Lawrence S. Kirschner,^{1,2} Donna F. Kusewitt,³ Ludmila Matyakhina,⁴ William H. Towns II,² J. Aidan Carney,⁶ Heiner Westphal,⁵ and Constantine A. Stratakis⁴

¹Human Cancer Genetics Program, ²Division of Endocrinology, Department of Internal Medicine, and ³Veterinary Biosciences Program, The Ohio State University, Columbus, Ohio; ⁴Section on Genetics and Endocrinology and ⁵Laboratory of Mammalian Genes and Development, National Institute of Child Health and Human Development, NIH, Bethesda, Maryland; and ⁶Department of Laboratory Medicine and Pathology, Mayo Clinic, Rochester, Minnesota

Abstract

Carney complex is an autosomal dominant neoplasia syndrome characterized by spotty skin pigmentation, myxomatosis, endocrine tumors, and schwannomas. This condition may be caused by inactivating mutations in *PRKARIA*, the gene encoding the type 1A regulatory subunit of protein kinase A. To better understand the mechanism by which *PRKARIA* mutations cause disease, we have developed conventional and conditional null alleles for *Prkar1a* in the mouse. *Prkar1a*^{+/-} mice developed nonpigmented schwannomas and fibro-osseous bone lesions beginning at ~6 months of age. Although genotype-specific cardiac and adrenal lesions were not seen, benign and malignant thyroid neoplasias were observed in older mice. This spectrum of tumors overlaps that seen in Carney complex patients, confirming the validity of this mouse model. Genetic analysis indicated that allelic loss occurred in a subset of tumor cells, suggesting that complete loss of *Prkar1a* plays a key role in tumorigenesis. Similarly, tissue-specific ablation of *Prkar1a* from a subset of facial neural crest cells caused the formation of schwannomas with divergent differentiation. These observations confirm the identity of *PRKARIA* as a tumor suppressor gene with specific importance to cyclic AMP–responsive tissues and suggest that these mice may be valuable tools not only for understanding endocrine tumorigenesis but also for understanding inherited predispositions for schwannoma formation. (Cancer Res 2005; 65(11): 4506-14)

Introduction

Carney complex (Online Mendelian Inheritance in Man 160987) is a multiple endocrine neoplasia syndrome characterized by spotty skin pigmentation, cardiac and extracardiac myxomatosis, schwannomas, and endocrine tumors (1). Specific examples of the latter include multiple hypersecretory adrenal nodules (described pathologically as primary pigmented nodular adrenocortical disease), growth hormone–secreting pituitary tumors, gonadal tumors, and thyroid neoplasias. The disease is inherited as an autosomal dominant trait (2), and there are two apparent loci that cause the same clinical syndrome (reviewed in ref. 1). We and others have shown previously that Carney complex may be caused by loss of function mutations in *PRKARIA*, which encodes the type

1A regulatory subunit of protein kinase A [PKA; cyclic AMP (cAMP)–dependent protein kinase; refs. 3–5]. Mutations in this gene are found in ~50% of affected kindreds, and sequence changes include nonsense mutations, frameshifts, and splice site alterations. Nearly all mutations described to date generate premature termination codons, and we have shown that these mutant mRNAs are degraded by the mechanism of nonsense-mediated mRNA decay (3). Functionally, loss of *PRKARIA* is associated with excess PKA signaling in tumors from patients (4), although the exact mechanism by which this aberrant signaling causes tissue-specific tumorigenesis is unknown. This question is particularly intriguing because activation of PKA has been shown to promote differentiation and block proliferation in many tissue culture systems (6–9), and PKA agonists have recently been proposed as useful agents for chemotherapy in leukemias (10). Because of the potential for unexpected effects of such a therapy, a thorough understanding of the consequences of PKA dysregulation is therefore critical.

From a genetic viewpoint, there have been conflicting reports on the role that loss of the normal allele of *PRKARIA* plays in Carney complex–associated tumorigenesis. Our work (4) has suggested that loss of heterozygosity (LOH) may be observed in a significant proportion of neoplasms, whereas other studies have not replicated this finding, particularly when studying cardiac or other myxomas (5, 11). LOH analysis and the finding of somatic mutations in sporadic thyroid and adrenal tumors support a role for complete loss of *PRKARIA* in tissue-specific tumorigenesis (12, 13).

To better understand the mechanism by which *PRKARIA* mutations cause disease, we have developed conventional and conditional null alleles for *Prkar1a* in the mouse. In this article, we report that mice heterozygous for a conventional null allele of *Prkar1a* (*Prkar1a*^{Δ2/+} mice) develop tumors in a spectrum that overlaps with those observed in Carney complex patients. We also present data aimed at determining the mechanism of tumorigenesis and show that tumor formation is recapitulated in mice with a tissue-specific knockout of the gene. These observations confirm the role of *PRKARIA* as a tumor suppressor gene with specific importance to cAMP-responsive tissues, such as Schwann cells, osteoblasts, and thyrocytes, and indicate that these mice will be valuable tools for modeling human tumor predispositions that affect these tissues.

Materials and Methods

Generation of a conditional allele for *Prkar1a*. To generate the *Prkar1a* targeting construct, a BAC clone containing the 5' end of the mouse gene was isolated from a commercially available library prepared from 129/Svj mice (Genome Systems, St. Louis, MO). The clones were

Requests for reprints: Lawrence S. Kirschner, Human Cancer Genetics Program, The Ohio State University, TMRF 544, 420 W 12th Ave., Columbus, OH 43210. Phone: 614-292-1190; Fax: 614-688-4006; E-mail: Kirschner-1@medctr.osu.edu.

©2005 American Association for Cancer Research.

isolated using primers from exon 2 (forward primer GAACCATGGCGTCTGG-CAGT and reverse primer AAGGAATGCCATGGGCTCT). Restriction mapping and subcloning of the BAC led to the isolation of 7.3-kb *Hind*III fragment and an overlapping 3.7-kb *Xba*I fragment containing the 5' end of the gene, including the promoter, the five alternatively spliced first exons (14), and the second exon. After sequencing and restriction mapping, a 3.4-kb *Bam*HI fragment corresponding to the promoter and the two potential first exons (exons 1a and 1b) of *Prkar1a* was cloned upstream of a *loxP* site, behind which was cloned the 3' adjacent 3.6-kb *Bam*HI fragment, containing other potential exons 1c, 1d, 1e, and 2. The resulting fragment was joined with a second clone carrying a *loxP*-NEO-*loxP* cassette, a 2.3-kb *Hind*III fragment of *Prkar1a* intron 2, and a HSV-TK cassette. The plasmid was linearized and electroporated into the R1 line of ES cells (15). Cells were double selected with G418 (350 μg/mL) and gancyclovir (2 mmol/L), and surviving clones were characterized at the 3' end by Southern blotting with a probe outside the flanking homologous sequences (Fig. 1A). Clones that exhibited the proper-sized fragment at the 3' end were further characterized by probing with a 5' end probe to verify proper homologous gene targeting (data not shown).

ES cells from two properly targeted colonies were injected into blastocysts, and six chimeras were identified, two of which transmitted the targeted flox-NEO allele (*Prkar1a*^{FN}) as judged by Southern and PCR analysis of tail DNA (Fig. 1B). For subsequent genotyping, tail DNA from mice was collected and analyzed by PCR. Primers and conditions for the PCR reactions are available upon request. The *Prkar1a*^{Δ2} and *Prkar1a*^{loxP}

alleles were generated from the *Prkar1a*^{FN} allele by crosses with the mosaic deleter strain *EIIA-cre* (16) as described in the text. For the generation of congenic mice, inbred mouse strains were obtained from Harlan (Indianapolis, IN) or The Jackson Laboratory (Bar Harbor, ME). All animal work in this study was carried out in accordance with Institutional Laboratory Animal Care and Use Committee guidelines under animal protocols 01-003 (at the NIH, Bethesda, MD) and 02-A-0097 (at The Ohio State University, Columbus, OH).

Southern and Western blotting. Genomic DNA (10 μg) was digested with *Eco*RV and separated on a 1% agarose gel. After transfer to nylon membranes (Genescreen Plus, Dupont-NEN, Boston, MA), samples were probed with a ³²P-labeled 1.2-kb *Pst*I fragment from the 3' end of the targeted construct. For Western blotting, proteins from cells were separated in 10% SDS-PAGE gels, transferred to nitrocellulose, and probed with monoclonal antibodies to Prkar1a or Prkar2a at dilutions recommended by the manufacturer (BD Biosciences, San Jose, CA). Western blots were developed using the Western Lightning Chemiluminescence Reagent as directed by the manufacturer (Perkin-Elmer Life Sciences, Inc., Boston, MA).

Analysis of tumors. Tissues were removed from mice, fixed in formalin, and stained with H&E. For immunohistochemical analysis, the following antibodies were used: S-100 (DAKO, Carpinteria, CA), keratin-14 (DAKO), neuron-specific enolase (NSE; DAKO), glial fibrillary acidic protein (GFAP; DAKO), and osteocalcin (Biomedical Technologies, Stoughton, MA). For S-100 and osteocalcin staining, samples were subject to antigen retrieval by steaming 20 minutes in Target Retrieval Solution (DAKO), whereas staining

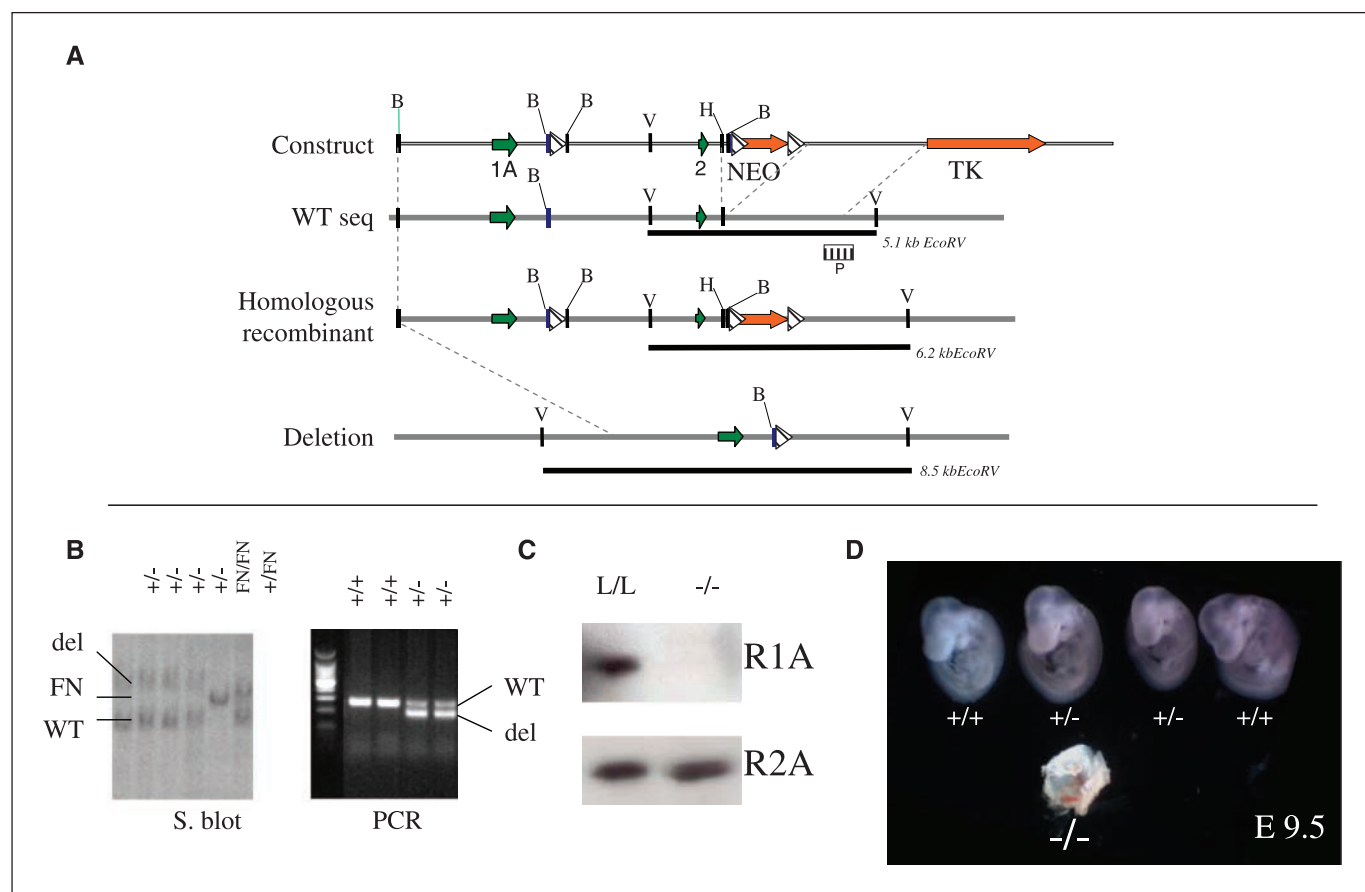


Figure 1. Generation of a null allele for *Prkar1a*. **A**, scheme for the generation of an allele of *Prkar1a* lacking exon 2 ($\Delta 2$). Green arrows, exons; hatched triangles, *loxP* sites; NEO, PGK-NEO cassette for positive selection; TK, thymidine kinase cassette included for negative selection; striped bar labeled P, probe used for Southern blotting. Selected restriction enzyme sites are also shown (B, *Bam*HI; V, *Eco*RV; H, *Hind*III). **B**, genotyping of mice by Southern blot using the probe indicated in (A; left) and genotyping of deletion mice by PCR (right). FN, flox-NEO allele; del or -, $\Delta 2$ allele; top, mouse genotypes. **C**, verification that the $\Delta 2$ allele is a null allele by Western blotting of *Prkar1a*^{loxP/loxP} (L/L) and *Prkar1a*^{Δ2/Δ2} (-/-) mouse embryonic fibroblasts with antibodies for Prkar1a (R1A) and Prkar2a (R2A). **D**, confirmation of early lethality of *Prkar1a* null embryos before E9.5. Genotypes of the embryos are shown. Note that heterozygote embryos are phenotypically normal.

for the other antigens was done without antigen retrieval. All slides were developed with Vector Elite ABC reagents (Vector Laboratories, Burlingame, CA). For fluorescence *in situ* hybridization (FISH) analysis, tumors were snap frozen in isopentane/liquid nitrogen, and touch preps were prepared on thawed samples. FISH was done as described (17) using a mouse BAC containing the entire *Prkar1a* gene.

Results

Generation of conventional and conditional null alleles for *Prkar1a*. To characterize the basis for *PRKARIA*-associated tumorigenesis in an animal model, we generated mice carrying a floxed copy of exon 2 of the murine *Prkar1a* gene. This exon, which contains the initiator ATG codon, was selected because Carney complex patients frequently show mutations affecting exon 2 (3, 4). The targeting vector (Fig. 1A) contained a total of 9.3 kb of genomic DNA isolated from a mouse BAC carrying the entire *Prkar1a* gene (data not shown). The mouse *Prkar1a* gene has been shown to use five alternative noncoding first exons, designated as exons 1a to 1e (14), all of which were in the cloned DNA fragment. The targeting construct was genetically engineered to contain a 5' *loxP* site between exons 1b and 1c as well as a floxed neomycin resistance cassette that was located in intron 2 after homologous recombination. Mice carrying the targeted allele (*Prkar1a*^{lox-NEO}) were phenotypically normal and homozygotes exhibited no abnormalities up to 1 year of age (data not shown). However, owing to previously reported problems caused by the presence of the neomycin resistance cassette within genes (18), mice were crossed with the *EIIA-cre* line (16) to obtain mice carrying all possible alleles resulting from cre-mediated recombination (data not shown; ref. 19). This led to the isolation of both the deletion allele *Prkar1a*^{Δ2} and the cognate conditional allele *Prkar1a*^{loxP} (Fig. 1B). To verify that the *Prkar1a*^{Δ2} was in fact a null allele, *Prkar1a*^{loxP/loxP} mouse embryonic fibroblasts were prepared and treated *in vitro* with cre recombinase.⁷ After verification of the resulting *Prkar1a*^{Δ2/Δ2} genotype, proteins were Western blotted to show the complete absence of Prkar1a protein (Fig. 1C). In addition, *Prkar1a*^{Δ2/+} mice were intercrossed, and genotyping of the litters revealed no *Prkar1a*^{Δ2/Δ2} pups. Embryos were prepared at E9.5, and analysis of the litters showed that all *Prkar1a*^{Δ2/Δ2} embryos exhibited advanced stages of tissue breakdown (Fig. 1D), confirming that the *Prkar1a*^{Δ2} allele was embryonic lethal in the homozygous state. This embryonic lethality has been characterized previously in detail for a different null allele of *Prkar1a* (20). This observation, coupled with the *in vitro* data described above, indicates that the *Prkar1a*^{Δ2} allele is a null allele. Because of the close similarity between our homozygous null embryos and the previous report, we elected not to characterize the embryonic phenotype further but rather to focus the remainder of our efforts on analysis of the tumorigenic phenotype of the heterozygous mice.

Tumorigenesis observed in *Prkar1a*^{Δ2/+} mice. To determine if mice carrying *Prkar1a*^{Δ2/+} exhibited tumorigenesis in a pattern similar to human patients, mice were maintained in a pathogen-free environment without intervention. We observed the mice for up to 2 years, and information from 44 *Prkar1a*^{Δ2/+} mice and 22 age-matched controls is included in this report. Visible solid tumors were commonly observed in *Prkar1a*^{Δ2/+} mice of 8 to 12 months of

age, although they were seen as early as 5 months and as late as 21.5 months (Table 1). In rare cases, the tumors had a s.c. cystic component adherent to the mass (data not shown). The most common location for these lesions was on the proximal hind limb (Fig. 2A), although they were also seen elsewhere, including the forelimb, head, and paw (Figs. 2B and 5D). For the majority of these tumors, histopathologic examination revealed that they were moderately cellular and composed of interlacing bundles of parallel spindle cells (Fig. 2C). Tumor cells exhibited modest pleiomorphism, although mitotic figures and nuclear palisading were rare. Scattered throughout the tumors were large cells containing variably sized highly eosinophilic cytoplasmic granules with an appearance consistent with hypertrophic Schwann cells (Fig. 2C). Immunohistochemical analysis (Fig. 2D-F) showed diffuse S-100 staining and patchy staining for NSE and GFAP. Based on these characteristics, these tumors were classified as schwannomas according to the recent criteria for the diagnosis of these tumors in genetically modified mice (21). Unlike patients with Carney complex, these typical schwannomas observed in the *Prkar1a*^{Δ2/+} mice did not exhibit melanotic pigmentation. In mice that developed tumors on the paws, the lesions had a somewhat different histopathologic appearance, but still met diagnostic criteria for schwannomas, albeit with divergent differentiation (21). This issue is discussed further below. Overall, schwannomas were observed in 33% of mice (14 of 44), making them the most frequent tumor necessitating euthanasia of the animals.

A striking feature of the *Prkar1a*^{Δ2/+} mice was the development of multiple tail tumors as shown in Fig. 3. These lesions first appeared at ~5 to 6 months of age. About 50% of *Prkar1a*^{Δ2/+} mice exhibited the lesions by 8 months, and the incidence rose to 80% at 1 year (Table 1). Radiographs of the tails (Fig. 3C) revealed radiolucent lesions, suggesting loss of normal bone. This process seemed to affect individual vertebrae and was not a field defect. Intriguingly, these lesions were observed only in the tail vertebrae of the mice and were not observed either grossly or radiographically in vertebrae proximal to the pelvis or in the long bones. Histologically (Fig. 3D), the lesions showed effacement of normal bone architecture with extensive remodeling, sometimes including expansion of the cortex. Disordered spindled cells, polygonal cells, stellate cells, and inflammatory cells embedded in abundant matrix replaced the normal bone trabeculae and filled the marrow cavity. Many of the abnormal polygonal cells associated with islands of bone stained positively for osteocalcin, identifying their osteoblastic lineage (Fig. 3D). These lesions in the *Prkar1a*^{Δ2/+} mice exhibit histologic similarity to osteochondromyxomas, a bony lesion that has been associated with Carney complex (22). Although lesions in patients usually occur in the nasal sinuses (in contrast to the tail tumors seen in mice), both lesions share a similar mixed pathology, including myxomatous, cartilaginous, and bony differentiation.

In addition to these externally obvious tumors, thyroid neoplasms were found in ~11% of *Prkar1a*^{Δ2/+} mice (5 of 44), although all were seen in mice older than 13.5 months (Fig. 3E-G; Table 1). One mouse exhibited multifocal tumors, as a follicular adenoma was found in one lobe and a solid-pattern thyroid carcinoma in the contralateral lobe. The cancers in these mice exhibited a solid pattern of growth (Fig. 3F), although some also had papillary elements. The diagnosis of carcinomas was based on the presence of capsular or vascular invasion as shown in Fig. 3G. As far as we are aware, these mice represent the first tumor suppressor gene knockout mouse model that spontaneously develops epithelial thyroid cancer.

⁷ K.S. Nadella and L.S. Kirschner, in preparation.

Other tumors observed only in *Prkar1a*^{A2/+} mice included pituitary chromophobe adenoma, pancreatic adenocarcinoma, thymoma, and bronchioloalveolar carcinoma (data not shown). The numbers of these tumor types were too small to determine if this was a genotype specific effect. No genotype-specific lesions were observed in the adrenal glands, the gonads, or the heart, and no pigmentary abnormalities were noted, although the *Prkar1a*^{A2} allele was carried into strains of various coloration. Cardiomyopathy, lymphoproliferative disease, and subcapsular nodular adrenocortical hyperplasia was observed in older knockout mice, but similar pathology was also seen in littermate controls, making these findings appear to be age-related but not genotype-related. The incidence of these findings was similar to what has been reported in phenotypic analysis of a variety of mouse strains used for cancer research (23).

To enhance the tumorigenic phenotype, we attempted to generate congenic mice in two different tumor prone strains, C3H and A/J (24). After three to four generations of inbreeding, animals (both males and females) of either congenic line were sterile, rendering further characterization impossible. Similar observations have been reported for efforts to breed *Prkar1a*^{+/-} mice in a C57BL/6 congenic background, although in that case sterility was only observed in male mice (25). Grossly, mice with significant genetic contribution from the C3H line exhibited an increased tendency to form bony lesions, with lesions involving the majority of the bones of the tail (data not shown). However, due to the limited breeding, no further observations could be made regarding genetic modifier loci in our study.

Allelic loss and tumorigenesis in *Prkar1a*^{+/-} mice. To address the question of the role of *Prkar1a* allelic loss in tumor formation in

Table 1. Tumors observed in *Prkar1a*^{A2/+} mice

Mouse ID	Sex	Age (mo)	Tumor	Tail	Schwannoma	Thyroid	Other
L2086	F	4.9	+	+	+		
L1702	M	5.6	+	-	+		Pancreatic tumor with mesenteric lymph node
L1554	F	6.0	-	-			
L2061	F	6.1	-	-			
L1553	F	6.3	+	+			Endometrial hyperplasia
L767	M	6.5	+	+			Carcinoma of unknown primary
2720	M	6.7	+	-			Extramedullary hematopoiesis
988	M	6.7	+	+	+		Extramedullary hematopoiesis
L786	F	6.9	+	+			
693	F	7.4	+	-	+		
L1649	M	8.1	+	+	+		
L1550	F	8.2	-	-			
U062904	F	8.4	+	+			
L1524	M	8.4	+	+			
L1515	M	8.5	+	+			Mesenteric carcinoma
L776	M	8.7	+	+			
U082504	F	9.3	+	+	+		
1204	F	9.5	+	+	+		
HLRI104	M	9.8	-	-			
L1651	M	10.0	+	+			
L2068	M	10.2	-	-			
L1513	M	10.3	+	+			Mesenteric mass (cystic)
U080504	F	11.4	+	+			
695	M	11.6	+	-	+		
L789	F	11.8	+	+			
L1650	M	11.9	+	+			
1882	F	12.7	+	+	+		
OH-1	M	13.0	+	-	+		Thymoma
C3H	M	13.3	+	+			
L510	M	13.3	+	-			Pancreatic tumor
L790	F	13.3	+	+			
L1214	M	13.3	-	-			
L488	F	13.4	+	+	+		
L142	F	13.5	+	-		Carcinoma	
HT100504	M	13.6	+	+	+	Carcinoma	
2816	M	13.9	+	+	+		
RL100504	F	14.9	+	+	+	Bilateral (adenoma, carcinoma)	
1658	M	17.7	+	+			
2718	M	18.6	+	+			
2730	M	18.6	+	+			
978	F	21.5	+	+	+	(Atypical) Adenoma	Lymphoproliferative disease
318	F	23.9	+	+			Bronchioloalveolar carcinoma, pit adenoma
290	F	24.3	+	+	+	(Usual, atypical) Carcinoma	
974	F	24.9	+	+			Endometrial hyperplasia

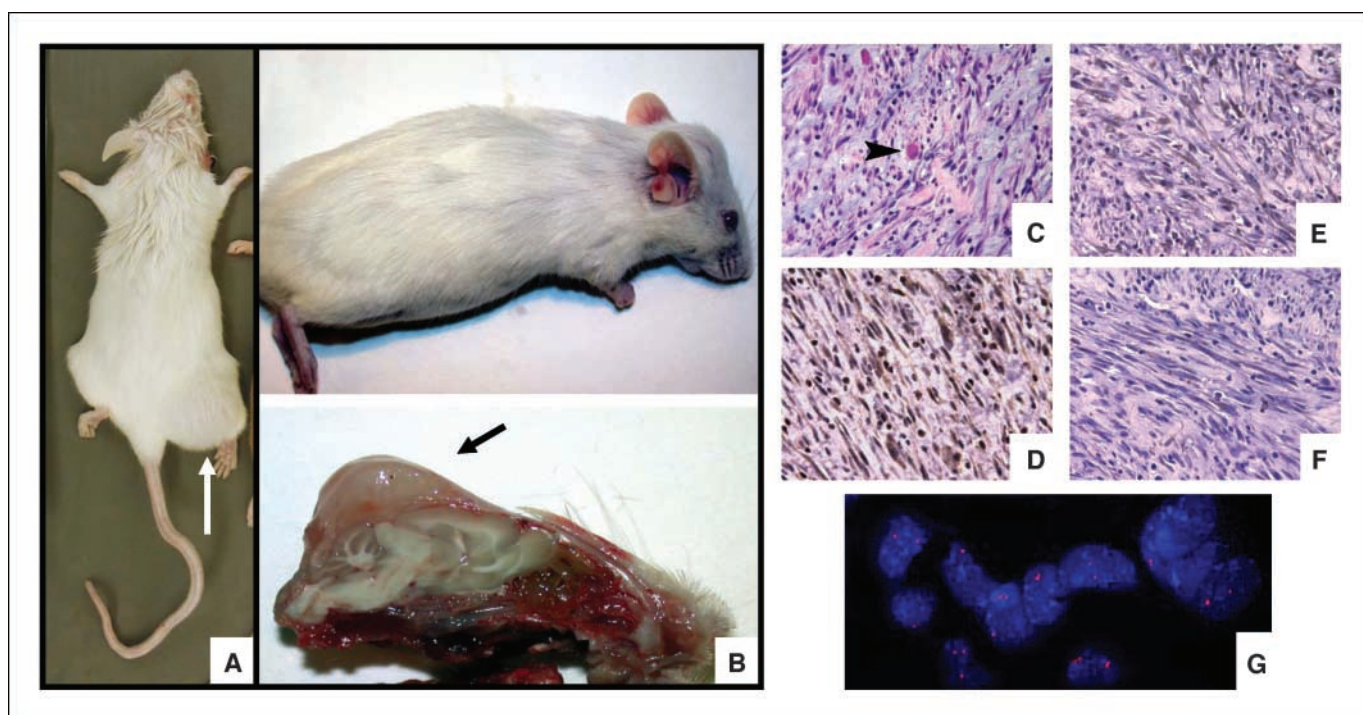


Figure 2. Schwannomas in *Prkar1a*^{A2/+} mice. The tumors were observed most frequently on the hind limb (A) but were also seen in other areas, including intracranially (B). C-F, microscopic and immunohistochemical findings from the tumors that are characteristic of schwannomas. C, H&E staining. Note the presence of granular cells with eosinophilic cytoplasmic granules (arrowhead) in a spindle cell background. D, diffuse strong staining of spindle cells for S-100. E, patchy staining of spindle cells for NSE. F, patchy staining of spindle cells for GFAP. G, FISH analysis showing allelic loss of the *Prkar1a* locus in approximately one third of cells. Red, *Prkar1a* BAC probe; blue, 4',6-diamidino-2-phenylindole–stained nuclei. Note the presence of multiple cells with only one signal, indicating allelic loss at this locus.

the mice, schwannoma samples were snap frozen and subsequently analyzed at the single-cell level by FISH. This analysis showed allelic loss at the *Prkar1a* locus at a rate of 30% to 50% (Fig. 2G). A similar analysis of the bone tumors showed allelic loss at a rate of 15% to 20% (data not shown). However, these numbers may underestimate the true rate of *Prkar1a* gene loss, as it was not possible to obtain a pure population of tumor cells in these experiments.

Tumorigenesis caused by tissue-specific loss of *Prkar1a*.

To assess directly the contribution of complete loss of *Prkar1a* to tumorigenesis, mice carrying the *Prkar1a*^{loxP} allele were bred to mice of the *TEC3* line, which express the cre recombinase in a subset of facial neural crest cells (26). Mice of the *TEC3;Prkar1a*^{loxP/loxP} genotype were born at the expected frequency and were fertile. Beginning ~3 to 4 months, mice developed unilateral or bilateral tumors on the lateral aspects of the face (Fig. 4). These tumors were not observed in *TEC3;Prkar1a*^{loxP/+} mice up to 18 months, providing strong genetic evidence that tumorigenesis is the result of complete loss of *Prkar1a* from targeted cells, although crude lysates of the *TEC3;Prkar1a*^{loxP/loxP} tumors showed immunoreactive Prkar1a protein (data not shown). Anatomically, the tumors arose in s.c. tissue lateral to the orbit and did not appear to involve overlying skin. Grossly, the tumors were fleshy and multilobulated, with an appearance similar to that of the schwannomas with divergent differentiation observed on the paws of *Prkar1a*^{A2/+} mice (Fig. 4).

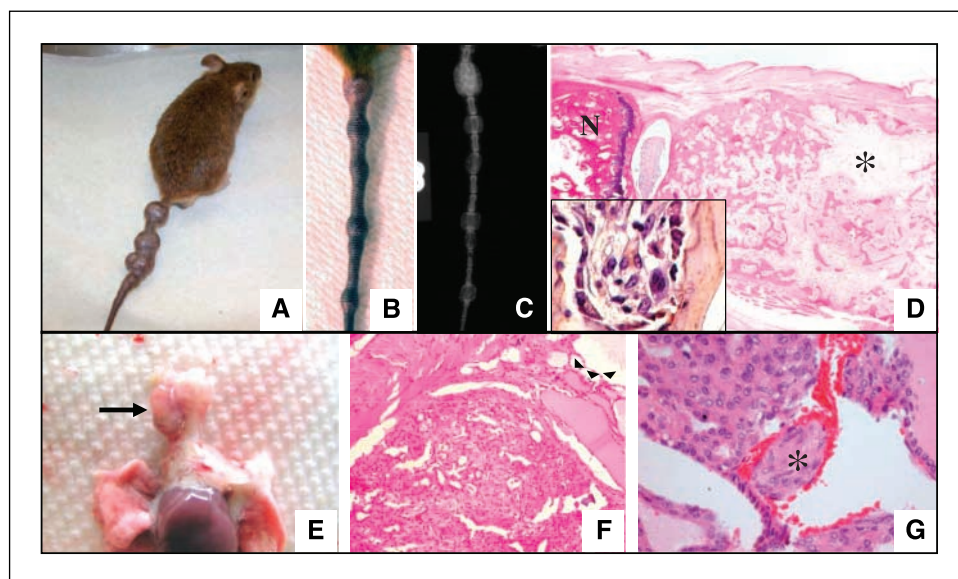
The tumors were composed primarily of spindle cells (Fig. 5A), with regions of neoplastic tubules and islands of neoplastic epithelial cells scattered throughout the tumors (Fig. 5B and C). Spindle cells were largely S-100 positive (Fig. 5D-F), whereas epithelial cells and tubules were keratin-14 positive (Fig. 5G and H). Cells transitional between these two cell types were also evident.

Small numbers of GFAP-positive cells were scattered irregularly through the masses; NSE-positive cells were not identified (data not shown). These tumors, like the histologically similar paw tumor seen in a *Prkar1a*^{A2/+} mouse (Figs. 4D and 5I-K), are therefore also classified as schwannomas, although these cellular elements indicate that they exhibit aspects of divergent differentiation, as has been seen in other mouse models involving schwannomas (21).

Discussion

We present here a detailed characterization of a mouse model for the human syndrome Carney complex by describing the phenotype of *Prkar1a*^{A2/+} mice. Although the spectrum of tumors observed in the mice is somewhat different from those observed in human patients, there is substantial overlap, as we have observed schwannomas, bone tumors, and thyroid neoplasms, all of which are observed in Carney complex patients (1). Our results differ significantly from a previously reported knockout mouse model whose most prominent features were hemangiosarcomas and other sarcomas (25, 27). A comparison of the constructs shows that the previous model targeted exons 3 to 5 (20), whereas ours targets exon 2. However, the differences in the observed phenotype are likely not due to functional differences in the resultant proteins (e.g., hypomorphic or dominant-negative alleles), as both alleles are associated with a complete lack of protein production (Fig. 1C; ref. 20). In fact, on detailed review, it is possible that some of the tumors classified as “myxoid fibrosarcomas” or “soft-tissue sarcomas” in the other model would meet our diagnostic criteria for schwannomas, although immunohistochemical characterization of those tumors was not undertaken. The criteria used in the present article reflect

Figure 3. Bone and thyroid lesions from *Prkar1a*^{Δ2/+} mice. A-D, tail lesions in *Prkar1a*^{Δ2/+} mice showing advanced lesions (A) and tails at an earlier stage or tumor development (B). C, X-ray of the mouse shown in (B) showing destruction of normal calcified bone. D, longitudinal section of an affected mouse tail showing a normal vertebra (N) adjacent to an involved bone. Note the proliferation of abnormal cells in the setting of a myxomatous stroma (*). Inset, immunohistochemical staining of the lesion for osteocalcin showing that the abnormal cells are of osteoblast lineage. Normal osteoblasts seen bordering apparently unaffected bone were also stained (arrowheads). E-G, thyroid lesions in *Prkar1a*^{Δ2/+} mice. E, gross pathology of a thyroid carcinoma (arrow). F, H&E-stained sections of thyroid carcinomas with a predominantly solid growth pattern. Top right, residual thyroid follicles (arrowheads). G, higher magnification view showing a grouping of thyroid cancer cells within a blood vessel (*).



recent advances in the understanding of schwannomas in genetically modified mice, which may have slightly different characteristics than tumors that arise spontaneously (21).

Even with this consideration, however, certain differences remain in the type and distribution of tumors observed. The reason for this discrepancy is unclear but may be due to strain differences. The prior model was generated in the C57BL/6 background, whereas our mice are of mixed background composed of 129/SvJ, C57BL/6, and FVB strains although with a >50% contribution from FVB. A small number (<10%) of the mice in this report also have contribution from the C3H strain, although this subgroup behaved similarly to the others with the exception of more aggressive bone lesions. From our limited ability to generate congenic strains, it already seems clear that genetic modifier loci are important in the phenotype of *Prkar1a* heterozygous mice, just

as they are in humans. It is also possible that the smaller number of mice ($n = 17$) and the shorter timeframe (19 months) of the previous report caused the authors to miss lower frequency lesions that occur in older mice, such as thyroid cancer.

In addition to the knockout approach, we have also recently described an alternate means to *Prkar1a* down-regulation by generating mice carrying a tetracycline-regulated antisense transgene for *Prkar1a*. Down-regulation of *Prkar1a* was shown *in vitro* and *in vivo* at both mRNA and protein levels (28), and the mice were observed to develop thyroid hyperplasia similar to that observed in human patients (29). These mice were also prone to the development of lymphomas and sarcomas, although these tumors are not frequent in Carney complex patients, and their significance is unknown. Although this mouse model mice will be a valuable tool for certain studies, its complexity makes it difficult to compare to the data from the study described here.

Comparison of *Prkar1a*^{Δ2/+} mice to other models of schwannoma formation. The occurrence of schwannomas in our mice is intriguing, as Schwann cell proliferation is stimulated by cAMP (30). In fact, most protocols to grow Schwann cells *in vitro* require the addition of PKA-activating agents in the culture medium (31). To determine if there is strong evidence linking human schwannomas to loss of *PRKARIA*, we analyzed LOH in a sample of sporadic human schwannomas ($n = 8$). In this small sample set, we did not observe evidence for allelic loss at the *PRKARIA* locus.⁸ Like in patients with Carney complex, Schwann cell tumors are known to develop in patients with neurofibromatosis, either type I or II (32). In contrast to the observations reported in this article, conventional knockout mouse models for *Nf1* or *Nf2* do not develop schwannomas (33), although these tumors can be induced under certain conditions (see below). At the biochemical level, there are good data indicating that PKA has a close functional relationship with the protein products of both *Nf1* and *Nf2* genes, known as neurofibromin and merlin (or schwannomin), respectively. Functionally, mutation in *Nf1* leads to increased intracellular cAMP (34), and presumably to increased PKA activity, which would mimic the increased PKA activity seen

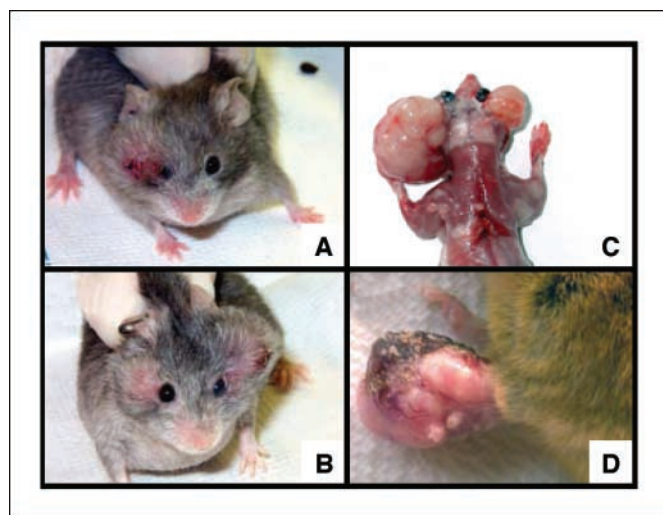


Figure 4. Tissue-specific ablation of *Prkar1a* leads to tumorigenesis. Mice of the *TEC3;Prkar1a*^{loxP/loxP} genotype developed unilateral (A) or bilateral (B) facial tumors at ~3 to 6 months of age. C, mouse in (B) following removal of skin, showing the heterogeneous lobulated nature of the bilateral tumors. D, a schwannoma with divergent differentiation arising on the paw of a *Prkar1a*^{Δ2/+} mouse. Histology of the tumors is shown in Fig. 5.

⁸ L.S. Kirschner, unpublished data.

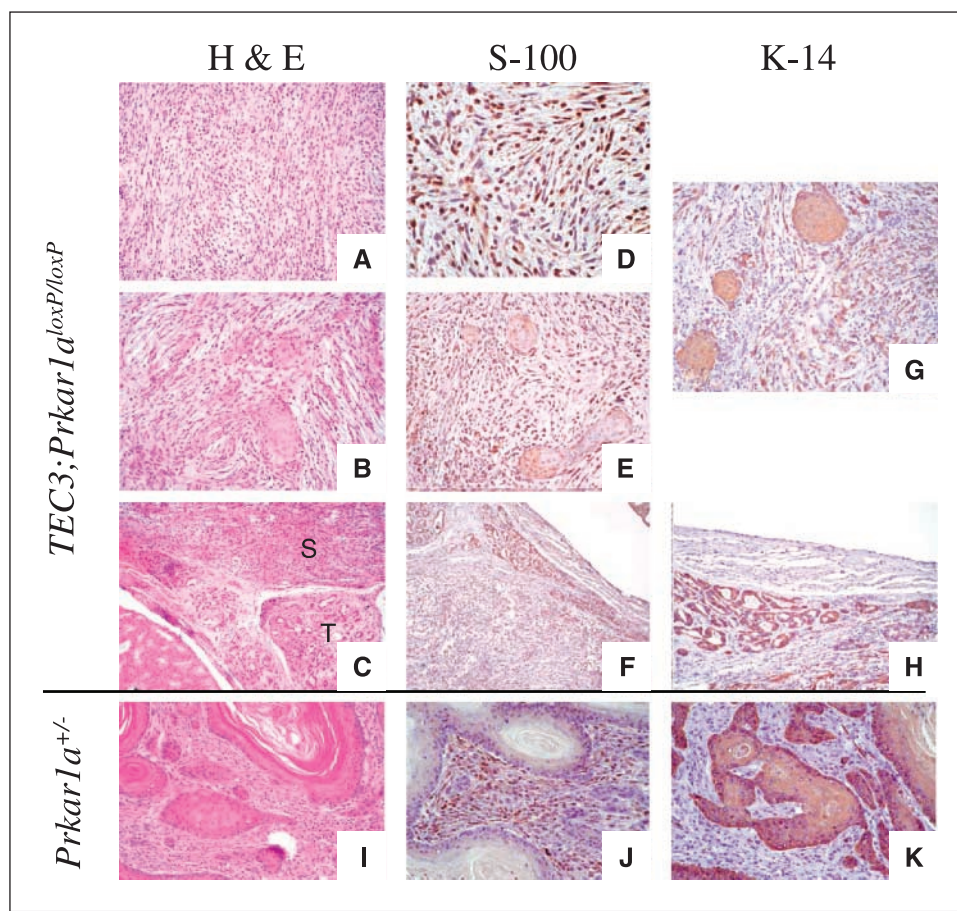


Figure 5. Comparison of schwannomas with divergent differentiation from *TEC3;Prkar1a^{loxP/loxP}* and *Prkar1a^{Δ2/+}* mice. A-C, H&E-stained tumor from a *TEC3;Prkar1a^{loxP/loxP}* mouse, showing spindle-shaped cells (A), islands of squamous epithelium embedded in the spindled cells (B), and neoplastic tubular epithelium (T) continuous with the spindle cell mass (S; C). D-F, S-100 staining of sections with similar histologic features. G and H, keratin-14 staining of spindle cells and epithelial islands (G) and neoplastic tubular cells (H). I, H&E staining of a schwannoma on the paw of a *Prkar1a^{Δ2/+}* mouse, showing islands of neoplastic epithelial tissue transitioning into spindle-shaped stromal cells. Staining of the same tumor for S-100 (J) and keratin-14 (K).

by loss of *Prkar1a* (4). PKA has also been shown to phosphorylate neurofibromin, although the functional consequences are currently unknown (35). Other studies have shown that PKA is able to phosphorylate merlin, and this post-translational modification blocks the growth-suppressive effects of merlin (36). In light of this close connection between control of PKA activity and *NF* gene function, the finding of frequent schwannomas in our mice is not unexpected. These observations suggest that the genetic interaction of *Prkar1a* with *Nf1* and *Nf2* bears further investigation, with the consideration that manipulation of the PKA system may provide a means to modify the phenotype of patients with neurofibromatosis.

Comparison of *Prkar1a^{Δ2/+}* bone lesions to those observed in patients with Carney complex or McCune-Albright syndrome. Although fibro-osseous lesions have been described as arising spontaneously in the bones of B6C3F1 mice (37, 38), the lesions observed in *Prkar1a^{Δ2/+}* mice exhibited distinct characteristics. First, these lesions were only observed in *Prkar1a^{Δ2/+}* mice, indicating that these abnormal growths were genotype specific. In B6C3F1 mice, lesions were typically observed in the sternum and femur and were not reported in the tail. In addition, those lesions exhibited a strong female predilection, which was not observed in the bone lesions of our mice (Table 1).

Dysplastic bone lesions are known to occur in Carney complex (22) and in another genetic condition, the McCune-Albright syndrome (MAS), in which case the lesions are described as fibrous dysplasia (32). This latter disease is due to activating mutations in the stimulatory G protein α -subunit (encoded by *GNAS1*) and also causes enhanced cAMP/PKA signaling (39). Like

in the *Prkar1a^{Δ2/+}* mice, the dysplastic bone seen in MAS is thought to result from a defect in osteoblast differentiation and/or proliferation (40), suggesting that the osteoblastic lineage is the target for genetic dysregulation of PKA signals in both of these conditions. Similar to Schwann cells, osteoblasts are known to have important physiologic responses to cAMP (41, 42), confirming the biological importance of this signaling pathway in this cell type. Given the fact that *GNAS1* lies upstream within the same pathway as PKA, it is not surprising that these two genetic defects may both produce bone abnormalities. However, although the lesions are similar, they can be distinguished based on their histopathologic appearance (43). In the bone lesions observed in *Prkar1a^{Δ2/+}* mice, the lesions were loose and relatively hypocellular compared with a greater cellularity in fibrous dysplasia. In addition, the former were composed largely of polygonal cells, whereas the latter exhibit spindled cell morphology. Finally, the bony trabeculae in our mice were rimmed by normal-appearing osteoblasts (Fig. 3D), a finding that is not observed in fibrous dysplasia. Thus, although the bone lesions of Carney complex and MAS appear similar, the abnormalities observed in our mice appear to correspond quite closely to the osteochondromyxomas seen in Carney complex, although they are clearly related, albeit at a greater distance, to the fibrous dysplasia observed in MAS.

Role of complete loss of *Prkar1a* in tumorigenesis. Finally, the question of the role of complete loss of *Prkar1a* in Carney complex tumors is not resolved by these studies, but our data suggest that this occurrence may be a key event in tumorigenesis. We base this conclusion on (a) the presence of allelic loss at the single-cell level in tumors (Fig. 2G), (b) the development of tumors

in the tissue specific knockout mice, and (c) the obvious similarity between tumors from tissue specific null and heterozygous mice. The fact that tumors do not seem to exhibit uniform allelic loss may suggest that loss of *Prkar1a* in a subset of cells is sufficient to cause tumorigenesis.

Intriguingly, similar observations have been made regarding the generation of Schwann cell tumors in neurofibromatosis. First, careful study of *NFI* patient tumors has shown that neurofibromas are composed of a mixture of Schwann cells that retain a functional *NFI* gene and those that have complete loss (44). As noted above, despite having nearly identical genetic defects, neurofibromas have not been observed in conventional *Nfi*^{+/-} mice (33). When *Nfi* was deleted from Schwann cells using a *Krox-cre* transgene with a conditional knockout allele (i.e., *Krox-cre;Nfi*^{loxP/loxP}), the mice also failed to develop significant tumors. However, when Schwann cells were made null for *Nfi* in the setting of *Nfi* heterozygosity (i.e., *Krox-cre;Nfi*^{loxP/-}), the mice developed schwannomas with 100% penetrance (45). The mechanism of this non-cell autonomous effect in *NFI*-mediated tumorigenesis has not yet been elucidated, but we hypothesize that a similar mechanism may be operating in both of these intersecting signaling pathways. This theory provides a good explanation for our current data and may also help explain some of the apparent discrepancies found in prior analyses of human tumors (4, 5, 11). Intriguingly, elegant studies on osteoblasts from fibrous dysplasia lesions have shown that transplantation of mutant osteoblasts did not recapitulate abnormal bone formation unless a coculture of normal and mutant osteoblasts was used (46). Although fibrous

dysplasia is caused by a dominant-activating mutation, the requirement for a mixture of genetically normal and abnormal cells shows that a similar non-cell autonomous phenomenon may be applicable.

Summary

Ultimately, the value of a mouse model for studying its associated human condition rests significantly in how well the mice develop tumors similar to those observed in human patients. *Prkar1a*^{Δ2/+} mice were generated to model the human syndrome Carney complex and are tumor prone. In contrast to a previous report, we find that these mice are a good model for Carney complex, developing tumors in highly relevant tissue, such as Schwann cells, osteoblasts, and thyrocytes. The availability of the *Prkar1a*^{loxP/loxP} mice should provide additional insights for studies of tissue-specific tumorigenesis and also to develop further data regarding the nature of the non-cell autonomous effects of *Prkar1a* loss.

Acknowledgments

Received 2/18/2005; accepted 3/16/2005.
Grant support: National Institute of Child Health and Human Development grant HD01323 (L.S. Kirschner) and National Cancer Institute grant CA16058 (The Ohio State University Comprehensive Cancer Center).
 The costs of publication of this article were defrayed in part by the payment of page charges. This article must therefore be hereby marked *advertisement* in accordance with 18 U.S.C. Section 1734 solely to indicate this fact.
 We thank Sara Lenherr for excellent technical assistance, Dr. Alex Grinberg for assistance with stem cell manipulation, Dr. Kurt Griffin for insightful discussion, and Drs. Ian Tonks and Graham Kay for providing the *TEC3* mice.

References

1. Stratakis CA, Kirschner LS, Carney JA. Clinical and molecular features of the Carney complex: diagnostic criteria and recommendations for patient evaluation. *J Clin Endocrinol Metab* 2001;86:4041-6.
2. Carney JA, Hruska LS, Beauchamp GD, Gordon H. Dominant inheritance of the complex of myxomas, spotty pigmentation, and endocrine overactivity. *Mayo Clin Proc* 1986;61:165-72.
3. Kirschner LS, Sandrini F, Monbo J, Lin JP, Carney JA, Stratakis CA. Genetic heterogeneity and spectrum of mutations of the PRKARIA gene in patients with the Carney complex. *Hum Mol Genet* 2000;9:3037-46.
4. Kirschner LS, Carney JA, Pack SD, et al. Mutations of the gene encoding the protein kinase A type I-α regulatory subunit in patients with the Carney complex. *Nat Genet* 2000;26:89-92.
5. Casey M, Vaughan CJ, He J, et al. Mutations in the protein kinase A RIα regulatory subunit cause familial cardiac myxomas and Carney complex. *J Clin Invest* 2000;106:R31-8.
6. Cho YJ, Kim JY, Jeong SW, Lee SB, Kim ON. Cyclic AMP induces activation of extracellular signal-regulated kinases in HL-60 cells: role in cAMP-induced differentiation. *Leuk Res* 2003;27:51-6.
7. Deebie PD, Murphy DJ, Parsons SJ, Cox ME. Interleukin-6- and cyclic AMP-mediated signaling potentiates neuroendocrine differentiation of LNCaP prostate tumor cells. *Mol Cell Biol* 2001;21:8471-82.
8. Han SY, Park DY, Lee GH, Park SD, Hong SH. Involvement of type I protein kinase A in the differentiation of L6 myoblast in conjunction with phosphatidylinositol 3-kinase. *Mol Cells* 2002;14:68-74.
9. Kim G, Choe Y, Park J, Cho S, Kim K. Activation of protein kinase A induces neuronal differentiation of HIB5 hippocampal progenitor cells. *Brain Res Mol Brain Res* 2002;109:134-45.

10. Weissinger EM, Oettrich K, Evans C, et al. Activation of protein kinase A (PKA) by 8-Cl-cAMP as a novel approach for antileukaemic therapy. *Br J Cancer* 2004;91:186-92.
11. Tsilou ET, Chan CC, Sandrini F, et al. Eyelid myxoma in Carney complex without PRKARIA allelic loss. *Am J Med Genet* 2004;130A:395-7.
12. Bertherat J, Groussin L, Sandrini F, et al. Molecular and functional analysis of PRKARIA and its locus (17q22-24) in sporadic adrenocortical tumors: 17q losses, somatic mutations, and protein kinase A expression and activity. *Cancer Res* 2003;63:5308-19.
13. Sandrini F, Matyakhina L, Sarlis NJ, et al. Regulatory subunit type I-α of protein kinase A (PRKARIA): a tumor-suppressor gene for sporadic thyroid cancer. *Genes Chromosomes Cancer* 2002;35:182-92.
14. Barradeau S, Imaizumi-Scherrer T, Weiss MC, Faust DM. Alternative 5'-exons of the mouse cAMP-dependent protein kinase subunit RIα gene are conserved and expressed in both a ubiquitous and tissue-restricted fashion. *FEBS Lett* 2000;476:272-6.
15. Nagy A, Rossant J, Nagy JS, Abramow-Newerly W, Roder JC. Derivation of completely cell culture-derived mice from early-passage embryonic stem cells. *Proc Natl Acad Sci U S A* 1993;90:8424-8.
16. Williams-Simons L, Westphal H. EIIaCre—utility of a general deleter strain. *Transgenic Res* 1999;8:53-4.
17. Matyakhina L, Pack S, Kirschner LS, et al. Chromosome 2 (2p16) abnormalities in Carney complex tumors. *J Med Genet* 2003;40:268-77.
18. Scacheri PC, Crabtree J, Novotny EA, et al. Bidirectional transcriptional activity of PGK-neomycin and unexpected embryonic lethality in heterozygote chimeric knockout mice. *Genesis* 2001;30:259-63.
19. Xu X, Li C, Garrett-Beal L, Larson D, Wynshaw-Boris A, Deng CX. Direct removal in the mouse of a floxed neo gene from a three-loxP conditional knockout allele by two novel approaches. *Genesis* 2001;30:1-6.
20. Amieux PS, Howe DG, Knickerbocker H, et al.

- Increased basal cAMP-dependent protein kinase activity inhibits the formation of mesoderm-derived structures in the developing mouse embryo. *J Biol Chem* 2002;277:27294-304.
21. Stemmer-Rachamimov AO, Louis DN, Nielsen GP, et al. Comparative pathology of nerve sheath tumors in mouse models and humans. *Cancer Res* 2004;64:3718-24.
22. Carney JA, Boccon-Gibod L, Jarka DE, et al. Osteochondromyxoma of bone: a congenital tumor associated with lentiginos and other unusual disorders. *Am J Surg Pathol* 2001;25:164-76.
23. Long P, Leininger J. Bone, joints and synovia. In: Maronpot R. Pathology of the mouse. Vienna (IL): Cache River Press; 1999. p.645-78.
24. Naf D, Krupke DM, Sundberg JP, Eppig JT, Bult CJ. The mouse tumor biology database: a public resource for cancer genetics and pathology of the mouse. *Cancer Res* 2002;62:1235-40.
25. Amieux PS, McKnight GS. The essential role of RIα in the maintenance of regulated PKA activity. *Ann N Y Acad Sci* 2002;968:75-95.
26. Tonks ID, Nurcombe V, Paterson C, et al. Tyrosinase-Cre mice for tissue-specific gene ablation in neural crest and neuroepithelial-derived tissues. *Genesis* 2003;37:131-8.
27. Veuglers M, Wilkes D, Burton K, et al. Comparative PRKARIA genotype-phenotype analyses in humans with Carney complex and *prkar1a* haploinsufficient mice. *Proc Natl Acad Sci U S A* 2004;101:14222-7.
28. Griffin KJ, Kirschner LS, Matyakhina L, et al. Down-regulation of regulatory subunit type 1A of protein kinase A leads to endocrine and other tumors. *Cancer Res* 2004;64:8811-5.
29. Griffin KJ, Kirschner LS, Matyakhina L, et al. A transgenic mouse bearing an antisense construct of regulatory subunit type 1A of protein kinase A develops endocrine and other tumours: comparison with Carney complex and other PRKARIA induced lesions. *J Med Genet* 2004;41:923-31.

30. Kim HA, DeClue JE, Ratner N. cAMP-dependent protein kinase A is required for Schwann cell growth: interactions between the cAMP and neuregulin/tyrosine kinase pathways. *J Neurosci Res* 1997;49:236-47.
31. Raff MC, Hornby-Smith A, Brookes JP. Cyclic AMP as a mitogenic signal for cultured rat Schwann cells. *Nature* 1978;273:672-3.
32. Online Mendelian Inheritance in Man [database on the Internet]. Baltimore: McLusick-Nathans Institute for Genetic Medicine, Johns Hopkins University and Bethesda: National Center for Biotechnology Information, National Library of Medicine; 2003. Available from: <http://www.ncbi.nlm.nih.gov/omim/>.
33. McClatchey AI, Cichowski K. Mouse models of neurofibromatosis. *Biochim Biophys Acta* 2001;1471:M73-80.
34. Kim HA, Ratner N, Roberts TM, Stiles CD. Schwann cell proliferative responses to cAMP and Nf1 are mediated by cyclin D1. *J Neurosci* 2001;21:1110-6.
35. Izawa I, Tamaki N, Saya H. Phosphorylation of neurofibromatosis type 1 gene product (neurofibromin) by cAMP-dependent protein kinase. *FEBS Lett* 1996;382:53-9.
36. Alftan K, Heiska L, Gronholm M, Renkema GH, Carpen O. Cyclic AMP-dependent protein kinase phosphorylates merlin at serine 518 independently of p21-activated kinase and promotes merlin-ezrin heterodimerization. *J Biol Chem* 2004;279:18559-66.
37. Albassam MA, Wojcinski ZW, Barsoum NJ, Smith GS. Spontaneous fibro-osseous proliferative lesions in the sternums and femurs of B6C3F1 mice. *Vet Pathol* 1991;28:381-8.
38. Sass B, Montali RJ. Spontaneous fibro-osseous lesions in aging female mice. *Lab Anim Sci* 1980;30:907-9.
39. Weinstein LS, Shenker A, Gejman PV, Merino MJ, Friedman E, Spiegel AM. Activating mutations of the stimulatory G protein in the McCune-Albright syndrome. *N Engl J Med* 1991;325:1688-95.
40. Riminucci M, Fisher LW, Shenker A, Spiegel AM, Bianco P, Gehron Robey P. Fibrous dysplasia of bone in the McCune-Albright syndrome: abnormalities in bone formation. *Am J Pathol* 1997;151:1587-600.
41. Romanello M, Moro L, Pirulli D, Crovella S, D'Andrea P. Effects of cAMP on intercellular coupling and osteoblast differentiation. *Biochem Biophys Res Commun* 2001;282:1138-44.
42. Swarthout JT, Tyson DR, Jefcoat SC Jr, Partridge NC, Efcoat SC Jr. Induction of transcriptional activity of the cyclic adenosine monophosphate response element binding protein by parathyroid hormone and epidermal growth factor in osteoblastic cells. *J Bone Miner Res* 2002;17:1401-7.
43. Riminucci M, Liu B, Corsi A, et al. The histopathology of fibrous dysplasia of bone in patients with activating mutations of the Gs α gene: site-specific patterns and recurrent histological hallmarks. *J Pathol* 1999;187:249-58.
44. Serra E, Rosenbaum T, Winner U, et al. Schwann cells harbor the somatic NF1 mutation in neurofibromas: evidence of two different Schwann cell subpopulations. *Hum Mol Genet* 2000;9:3055-64.
45. Zhu Y, Ghosh P, Charnay P, Burns DK, Parada LF. Neurofibromas in NF1: Schwann cell origin and role of tumor environment. *Science* 2002;296:920-2.
46. Bianco P, Kuznetsov SA, Riminucci M, Fisher LW, Spiegel AM, Robey PG. Reproduction of human fibrous dysplasia of bone in immunocompromised mice by transplanted mosaics of normal and Gs α -mutated skeletal progenitor cells. *J Clin Invest* 1998;101:1737-44.